Original Article

Role of autophagy in the periodontal ligament reconstruction during orthodontic tooth movement in rats

Jie Xu [a], Xian Zhao [a], Jin Zeng [a], Jing-Hong Yu [a], Simon Guan [b], Xiao-Mei Xu [a*], Li Mei [c]

[a] Department of Orthodontics, The Affiliated Stomatology Hospital of Southwest Medical University, Oral & Maxillofacial Reconstruction and Regeneration Laboratory, Southwest Medical University, Luzhou, Sichuan, PR China

[b] Department of Oral Diagnostic and Surgical Sciences, Faculty of Dentistry, University of Otago, New Zealand

[c] Discipline of Orthodontics, Department of Oral Science, Sir John Walsh Research Institute, Faculty of Dentistry, University of Otago, Dunedin, New Zealand

Background/purpose: Autophagy, a lysosome-based degradation pathway that is reportedly activated by mechanical stress and nutrient deprivation, plays an important role in various physiological and pathological events. The present study investigated the level of autophagy and tumor necrosis factor-α(TNF-α) expression in the periodontal ligaments (PDLs) of Sprague—Dawley (SD) rats to analyze the involvement of autophagy and inflammatory cytokines in orthodontic tooth movement (OTM) and maintaining periodontal tissue homeostasis.
Materials and methods: SD rats (n = 100) were randomly divided into a control group (n = 10) and an experimental group (n = 90). An orthodontic appliance was placed in each rat in the experimental group, and 10 rats were randomly euthanized 15 min, 30 min, 1 h, 2 h, 4 h, 12 h, 1 d, 3 d and 7 d after mechanical loading. The OTM distance was then measured. Hematoxylin and eosin (HE) staining was used to analyze the morphology of the PDL. Immunohistochemical (IHC) staining and tartrate-resistant acid phosphatase (TRAP) staining were also performed.
Results: After the application of orthodontic force and under the dual effects of mechanical force and starvation caused by compressed vessels, the level of autophagy and TNF-α expression in the PDL fluctuated and exhibited a similar trend.
Conclusion: Our data suggest a significant correlation between the initiation of autophagy and

* Corresponding author. Department of Orthodontics, The Affiliated Stomatology Hospital of Southwest Medical University, Oral & Maxillofacial Reconstruction and Regeneration Laboratory, Southwest Medical University, 2 Jiangyang South Road, Luzhou, Sichuan, 646000, PR China.
 E-mail address: xuxiaomei@hotmail.com (X.-M. Xu).

Introduction

Orthodontic tooth movement (OTM) is a process related to the continuous physiological response and adaptation of the periodontal tissue to an externally applied force. As the initial recipient of the orthodontic force, the periodontal ligament (PDL) is an important bridge through which the orthodontic force exerts a vital biological effect.[1] Mechanical force triggers various microscopic and macroscopic alterations in the PDL, mediating the remodeling of periodontal tissue. When the tooth to which an orthodontic force is applied begins to move beyond its original physiological location, the compression side of the PDL is appreciably deformed and compressed, while the tension side of the PDL is stretched.[2] Subsequently, the tissue fluid filling the PDL space begins to flow, deforming the periodontal ligament cells (PDLCs). Then, the mechanical-chemical transduction system is activated, resulting in the local synthesis and release of a variety of key cytokines and inflammatory mediators, triggering a series of tissue responses such as hyaline degeneration and osteoclast aggregation in the compression side of the PDL, bone resorption in the compression side of the PDL and bone formation in the tension side of the PDL, ultimately allowing tooth movement.[3] The reception, response and adaptation of PDLCs to mechanical stimulation during OTM suggest their vital functions in the reconstruction of periodontal tissue. How do PDLCs achieve an adaptive response to mechanical stress? The mechanisms underlying this response remain elusive.

PDLCs are located in a tridimensional microenvironment and are often subjected to multiple different types, values and directions of mechanical force.[4] Mechanical force experienced by the periodontal tissue structure and cell physiology are regulated throughout the entire life cycle of the organism. The adaptability of cells to changes in the mechanical environment is very important for maintaining cellular homeostasis and normal functioning. After an orthodontic force is applied to a tooth, an initial tipping movement occurs within the alveolar socket, and the PDLCs are subjected to compressive or tensile mechanical stress.[5] Concomitantly, blood vessels in the compression side of the PDL are compressed, which might create a "starvation" microenvironment. Thus, OTM induces mechanical stress and nutrient deprivation. Autophagy is a highly conserved catabolic mechanism. For many decades, researchers have known that autophagy occurs in a wide range of eukaryotic organisms and multiple different cell types during starvation, cellular and tissue remodeling, and cell death.[6-8] The autophagic response, which is part of an integrated response to mechanical challenge, allows cells to cope with a continuously changing physical environment.[9] Therefore, cell and tissue autophagy might have emerging importance in the reconstruction of periodontal tissue and cellular homeostasis during OTM. However, apoptosis is triggered in the presence of excessive or inhibited autophagy.[10-12] Cellular autophagy is described as comprising three phases. The initial stage involves the formation of autophagic vacuoles, which are double-membrane vesicles that package the remodeled subcellular membranes. Autophagic vacuoles then sequester damaged proteins or organelles, leading to the production of autophagosomes.[6] Finally, autophagosomes fuse with lysosomes to form autophagolysosomes, in which the cytoplasmic contents are degraded and recycled.[13] Light chain 3B (LC3B), beclin-1 and p62/sequestosome 1 (p62/SQSTM1) are three crucial proteins that monitor the formation of autophagosomes and autolysosomes.[14-17] Changes in the levels of these markers indicate alterations in autophagy (i.e., reduction, hyperactivation, or impairment).

In addition, autophagy is closely related to inflammation, which regulates cell death and inflammation. The induction of autophagy reportedly depends on the presence of the inflammasome sensor.[18,19] OTM is a sterile inflammatory process, and a relationship exists between inflammatory factors and periodontal tissue remodeling.[20] Based on the current evidence, we speculate that orthodontic forces and inflammatory cytokines induce autophagy in PDLCs and that autophagy plays a key role in the adaptation of PDLCs to mechanical stimulation and the inflammatory environment. Additionally, inflammatory cytokines may mediate cell autophagy induced by mechanical stimulation. This study summarizes the physiological roles and mutual relationship between autophagy and the inflammatory cytokine tumor necrosis factor-α(TNF-α) in mediating PDL reconstruction during OTM in rats to better explain the potential importance of autophagy in the adaptation of PDLCs to mechanical force and the inflammatory microenvironment during tooth movement.

Materials and methods

Laboratory animal model of OTM

Ethical approval for the present study was provided by the Ethics Committee (no. 201703026) of The Affiliated Stomatology Hospital of Southwest Medical University (Luzhou, China) on 26 March 2017. We used a rat OTM model to confirm the involvement of autophagy during periodontal tissue remodeling induced by mechanical loading (Fig. 1A). The experimental protocol for OTM was performed as previously described.[21] One hundred 6-8-week-old male Sprague—Dawley (SD) rats with a mean weight of 247 ± 33 g were used in the experiment. Animals were
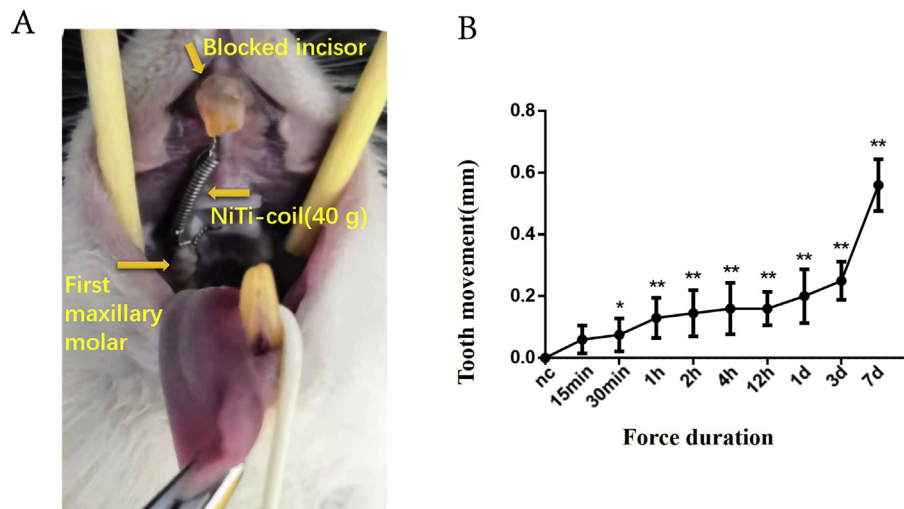
Fig. 1 Orthodontic tooth movement. A) Image of an inserted orthodontic appliance fixed between the blocked incisor and the first maxillary molar in an SD rat. The maxillary molar is drawn to the mesial side. B) OTM distance at different time points.

provided by the Experimental Animal Center of Southwest Medical University Authority, and animal procedures were conducted in accordance with the Animal Welfare Act. One hundred animals were housed under standard humidity, ventilation, temperature, and light conditions with food and water provided ad libitum. All rats were acclimated for one week prior to any experimental procedures. Ninety rats were included in the experimental group, and ten rats served as an unoperated control group. The animals in the experimental group were anesthetized with an intraperitoneal injection of chloral hydrate at a concentration of 0.1 g/ml and use of 4 ml per 1 kg body weight, that is 0.4 g chloral hydrate per 1 kg body weight. The anesthetized rats were placed in the dorsal decubitus position with their four limbs affixed to a surgical table. An orthodontic appliance was placed between the maxillary right first molar and central incisor of each rat in the experimental group under general anesthesia, and the maxillary right first molar was mesially moved by a coiled spring (IMB, Shanghai, China), delivering a force of 40 g. We prepared a 0.5-mm groove on the incisors in which the ligature wire was seated and secured it with a light-cured resin (Xihubiom, Hangzhou, China) to prevent the detachment of the appliance. Henceforth, the animals' food supply was ground to avoid possible damage to the orthodontic appliance. Each rat was checked daily to ensure that the spring remained in place, and if the spring fell off, the rat was immediately sacrificed, and the animal OTM model was reconstructed using another rat.

Conditions of the rats

During our 1-week experiment, the orthodontic appliances fell off in five of 90 rats, which were sacrificed and replaced by five other rats to ensure that ten rats were available for

the final analysis. No appreciable inflammatory response was observed at the local injection site in any of the 90 animals examined. The application of the orthodontic force did not affect the body weight of the rats.

Animal grouping and tissue preparation

The experimental animals were randomly divided into nine groups, to which 15 min, 30 min, 1 h, 2 h, 4 h, 12 h, 1 d, 3 d, or 7 d of force was applied. Animals were euthanized by an intraperitoneal injection of excessive chloral hydrate at each experimental time point. And rats have no heartbeat and both eyes are grayish white as the standards of death. The hemimaxillae were removed and fixed with a 4% paraformaldehyde (Biosharp, Anhui, China) solution, pH 7.4, for 48 h. Subsequently, the fixed tissues were decalcified by immersion in a 14% EDTA (Solarbio, Beijing, China) solution for 6–8 weeks. After complete decalcification, blocks of tissue containing the maxillary right first molar and the surrounding alveolar bone were dehydrated with a graded alcohol series and embedded in paraffin. The specimens were oriented in the paraffin blocks such that mesiodistal sections parallel to the long axis of the teeth were cut. Serial sections (4-μm-thick) were cut and mounted on glass slides.

Measurement of the OTM distance

We measured the bilateral distance from the most mesial point of the maxillary second molar to the most distal point of the first molar using electronic Vernier calipers to determine the OTM distance. The OTM distance was the difference between the experimental side and the control side. Each distance was measured twice by the same observer, and the mean value was used.
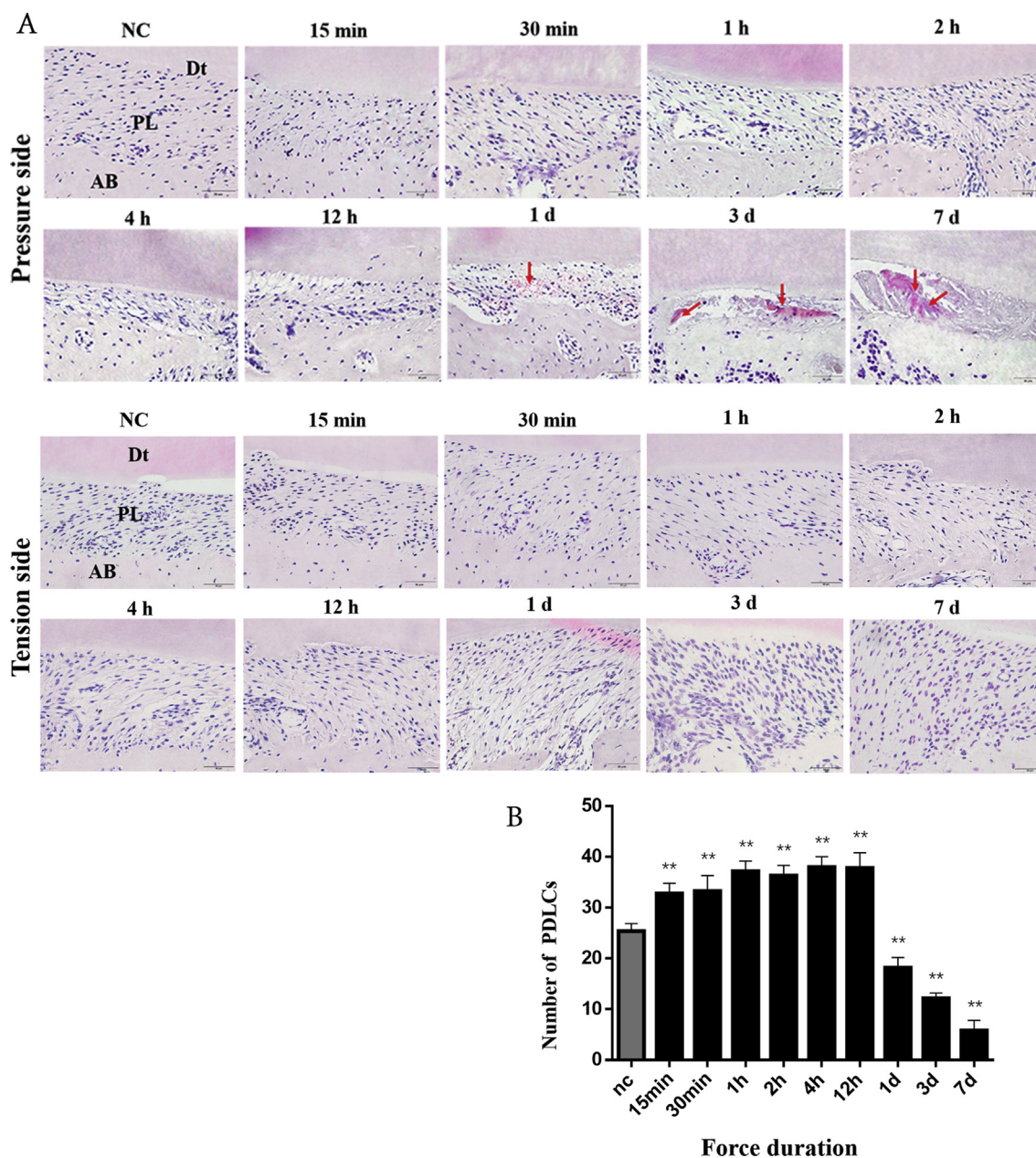
Fig. 2 HE staining of the pressure side and tension side of the periodontium at different time points. A) Representative images of HE staining. In the control group, the PDL was neatly arranged. At 1 d after OTM, the pressure side of the PDL was compressed and narrow, and hyalinization was observed. The tension side of the PDL was stretched and wider. AB, alveolar bone; Dt, dentin; PDL, periodontal ligament. Scale bars = 50 μm. B) Number of PDLCs in the compression side at different time points. The number of PDLCs gradually increased after the application of the orthodontic force compared to the control group, while the number of PDLCs began to decrease after the application of the orthodontic force for 1 d, with the lowest value observed after 7 d **$P < 0.01$, n = 10 animals per group.

Hematoxylin and eosin (HE) staining

Changes in periodontal tissue sections were examined using HE (Solarbio) staining under an optical microscope. Sections were deparaffinized with xylene three times (10 min each) and rehydrated through a graded alcohol series. After the slices were washed with double-distilled water (DDW) and dried, they were incubated with hematoxylin for 6 min, and then a 1% HCl alcohol solution was added for 10 s before rinsing with water. Slices were washed for 25 min and then incubated with 0.5% eosin for 6 min. After washes with phosphate-buffered saline (PBS), slices were sequentially dehydrated with 75%, 85%, 95% and 100% ethanol. Slices were incubated with dimethylbenzene three times for 2 min each, and the slices were mounted with neutral resins. First, the distal tension side of the molar mesial root
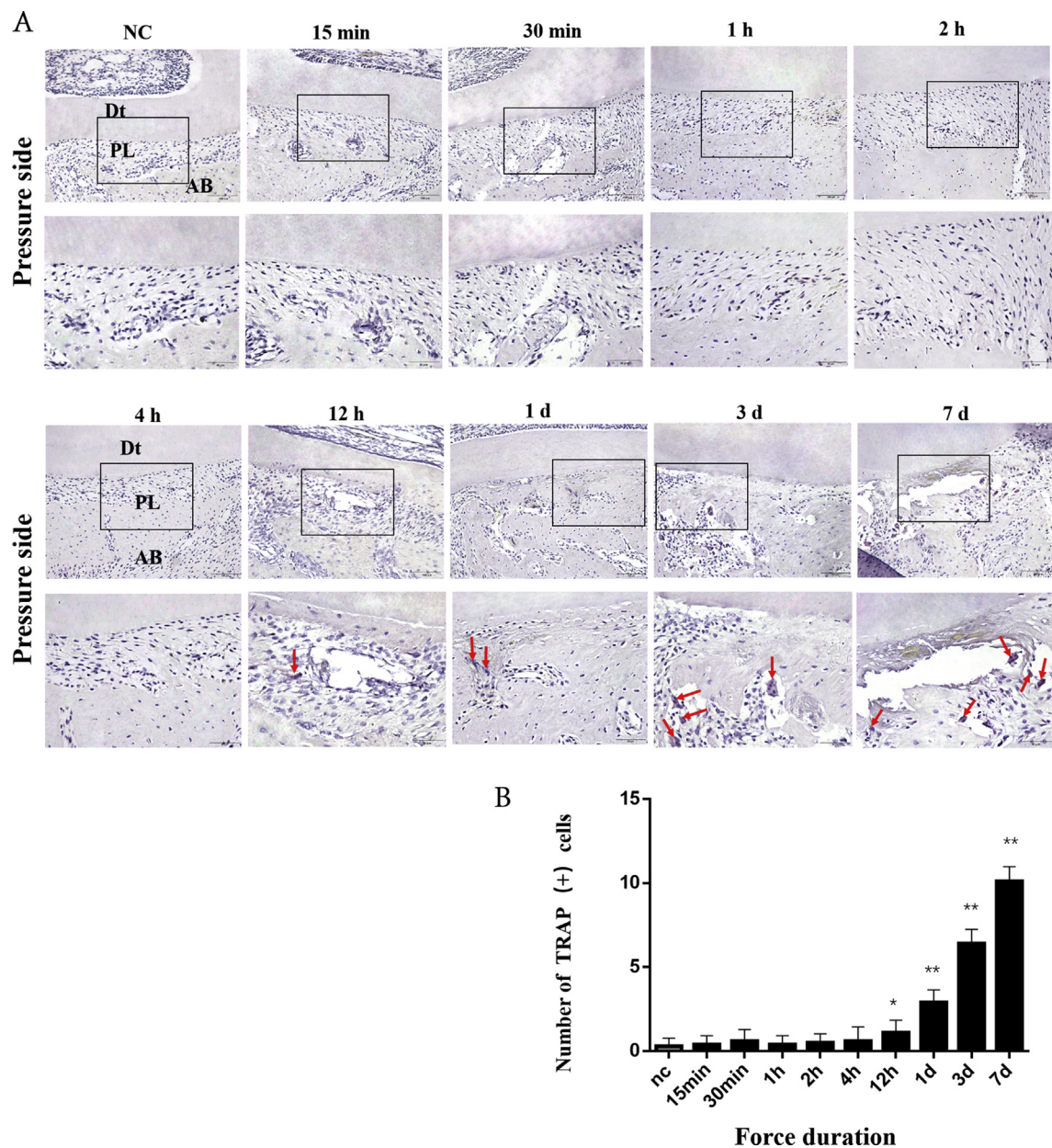
Fig. 3 TRAP IHC staining of the compression side at different time points. A) Representative images of TRAP IHC staining; higher magnification images of the squares in the images in the upper panels are shown in the lower panels. AB, alveolar bone; Dt, dentin. Red arrows: osteoclasts. B) Number of TRAP (+) cells. *P < 0.05, **P < 0.01, n = 10 animals per group.

and the mesial compression side of the distal root were observed under a light microscope, and the number of PDLCs in the compression side was counted using Image-Pro Plus 6.0 software (Media Cybernetics, Bethesda, MD, USA).

Tartrate-resistant acid phosphatase (TRAP) immunohistochemical (IHC) staining

For TRAP IHC staining, sections were immersed in xylene twice for 10 min each to eliminate paraffin, dehydrated in absolute alcohol, and rehydrated through a graded ethanol series to DDW. Activated osteoclasts were labeled by performing TRAP staining (Tartrate-resistant Acid Phosphatase

Assay, Beyotime, Shanghai, China). The total number of TRAP-positive osteoclasts at the PDL compression side on the distal buccal root of the first maxillary molar was counted under an optical microscope.

IHC staining for beclin-1, LC3B, p62/SQSTM1, CD34, and TNF-α

IHC staining was performed to detect the levels of the autophagy markers beclin-1, p62/SQSTM1 and LC3B, and vascular endothelial marker CD34, and evaluate the level of autophagy and microvessel density, respectively, in PDLs. Serial sections (5 μm) were deparaffinized, rehydrated,
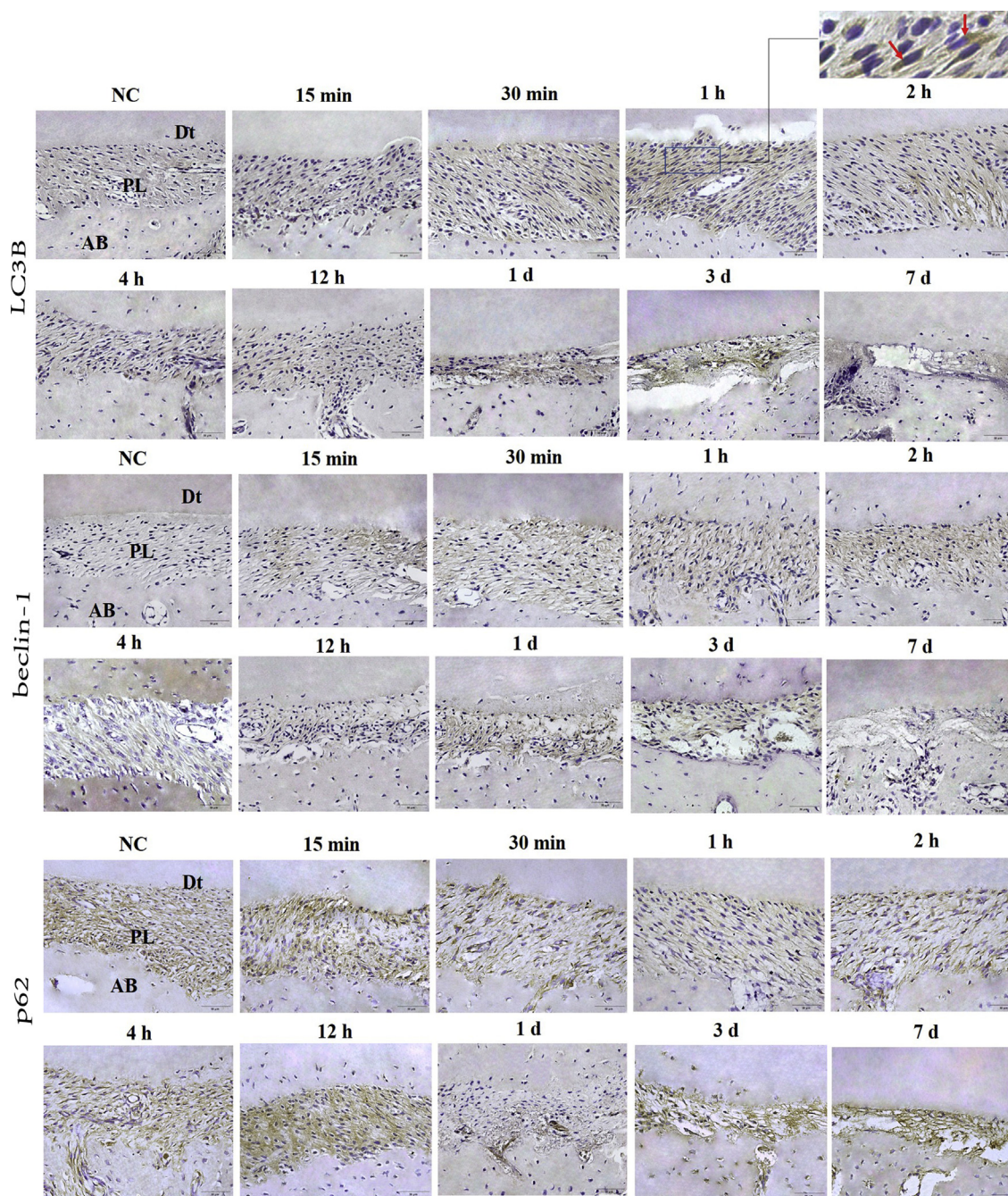
Fig. 4 IHC staining for beclin-1, LC3B and p62/SQSTM1 in the compression side at different time points. Scale bars = 50 μm. Since beclin-1, LC3B and p62/SQSTM1 are located in the cytoplasm, cells in which the nuclei were stained blue and cytoplasm was stained brown were considered positive. The higher magnification image of the square in the IHC staining image for LC3B at 1 h is shown in the upper right corner panel. Red arrows: the positive cells.

washed with distilled water, and then soaked in PBS for 5 min. These steps were followed by an incubation with a 3% hydrogen peroxide solution (SP-0023 Histostain-Plus Kit, Bioss, Beijing, China) for 20 min. Then, the sections were washed with PBS containing 0.1% Triton TM X-100.31 three times for 5 min each and blocked with normal goat serum (SP-0023 Histostain-Plus Kit, Bioss) for 20 min. The sections were incubated with the following primary antibodies in a humidified chamber overnight at 4 °C: 1) rabbit anti-beclin-

1 polyclonal antibody (Abcam, Cambridge, UK) diluted 1:1000, 2) rabbit anti-LC3B polyclonal antibody (Abcam) diluted 1:800, 3) rabbit anti-p62/SQSTM1 polyclonal antibody (Abcam) diluted 1:100, 4) rabbit anti-TNF-α polyclonal antibody (Abcam) diluted 1:100, and 5) rabbit anti-CD34 monoclonal antibody (Abcam) diluted 1:100. After rinses with PBS, the sections were incubated with a goat anti-rabbit secondary antibody (SP-0023 Histostain-Plus Kit, Bioss) for 20 min at room temperature and subsequently
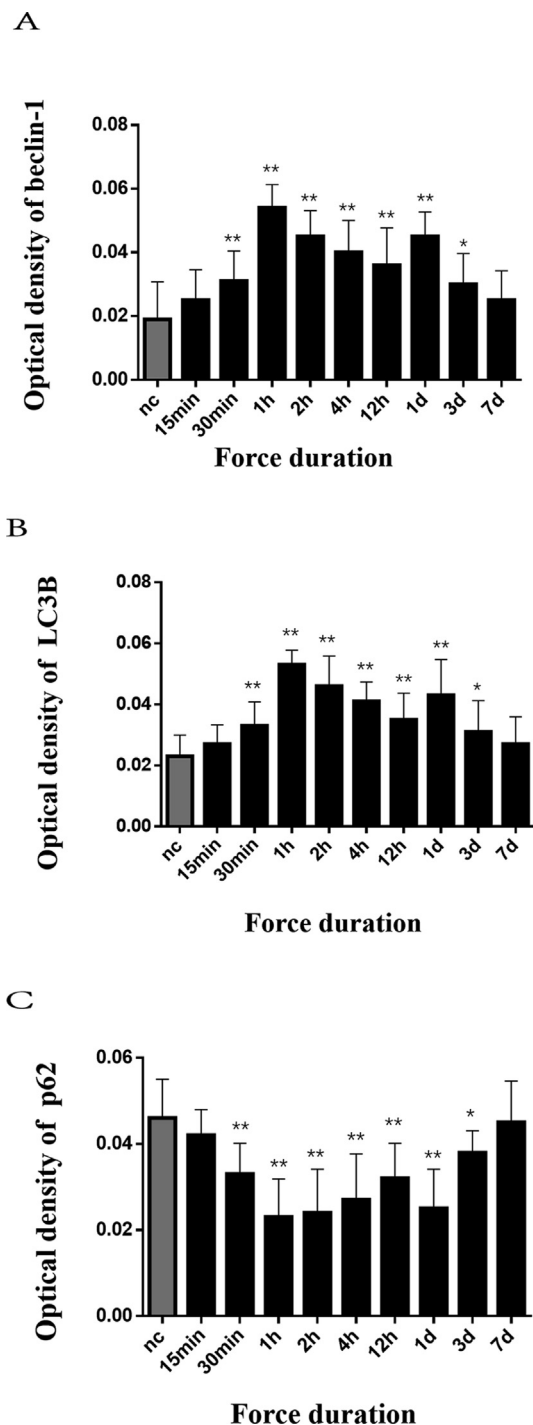
A

B

C

Fig. 5 Quantitative analysis of IHC staining for beclin-1, LC3B and p62/SQSTM1. *P < 0.05, **P < 0.01, n = animals 10 per group.

incubated with streptavidin horseradish peroxidase (SP-0023 Histostain-Plus Kit, Bioss) for 20 min at room temperature. Diaminobenzidine (DAB, Bioss) was used as a chromogen, and sections were counterstained with hematoxylin. After washes with PBS, the slices were sequentially dehydrated with 75%, 85%, 95% and 100% ethanol. Sections were incubated with dimethylbenzene three times for 2 min each, and the slices were mounted with neutral resins. Since beclin-1, LC3B and p62/SQSTM1

are located in the cytoplasm, cells in which the nuclei were stained blue and cytoplasm was stained brown were considered positive. Sections were observed under a light microscope at 400 × magnification. The quantitative analysis was performed using Image-Pro Plus 6.0 software (Media Cybernetics), and the integrated optical density (IOD) was used as an indicator of positive staining.

Statistical analysis

Data are presented as the mean ± standard deviation of ten independent experiments. Statistical analyses of data were performed using one-way analysis of variance with SPSS software (version 21.0; IBM, New York, USA) and GraphPad Prism software (version 6.0; GraphPad Software, Inc., La Jolla, CA, USA). P < 0.05 was considered to indicate a statistically significant difference. In addition, in all statistical analyses, the experimental groups were just compared with the negative control group. There was no pairwise comparison among the experimental groups.

Results

Measurement of the OTM distance

The OTM distance was proportional to the time of orthodontic force until 7 d, when the maximum OTM was observed. The OTM in the group exposed to orthodontic force for 30 min differed statistically from the control group, while tooth movement increased significantly at 1 h (P < 0.01), followed by unobvious tooth movement from 1 h to 12 h. The OTM distance increased again after the application of force for 12 h (Fig. 1B).

Histological changes in PDLs induced by mechanical stimuli, as examined using HE staining

Following HE staining, the histopathological examination indicated different changes in the PDL tissue structure following tooth movement for different periods of time (Fig. 2A). In the negative control group, the PDL was arranged in an orderly manner and exhibited no destruction. In the pressure area of the PDL in the experimental group, the PDL fibers were arranged irregularly and resembled wrinkles. Over time, the width of the PDL gradually decreased. At 1 d, hyalinization appeared in the PDL, and hyalinization in the PDL was widely distributed at 7 d. In the tension zone of the PDL, the PDL fibers were stretched, and the width of the PDL gradually increased. The number of PDLCs in the compression side gradually increased after the application of orthodontic force (P < 0.01) (Fig. 2B) and then remained stable from 1 h to 12 h. The number of PDLCs decreased quickly after 12 h (P < 0.01) and was below the basal level at 7 d (P < 0.01).

TRAP IHC staining of the compression side

TRAP-positive cells mainly appeared around areas of hyalinization and near the alveolar bone (Fig. 3A). The number of TRAP-positive osteoclasts in the compression side was
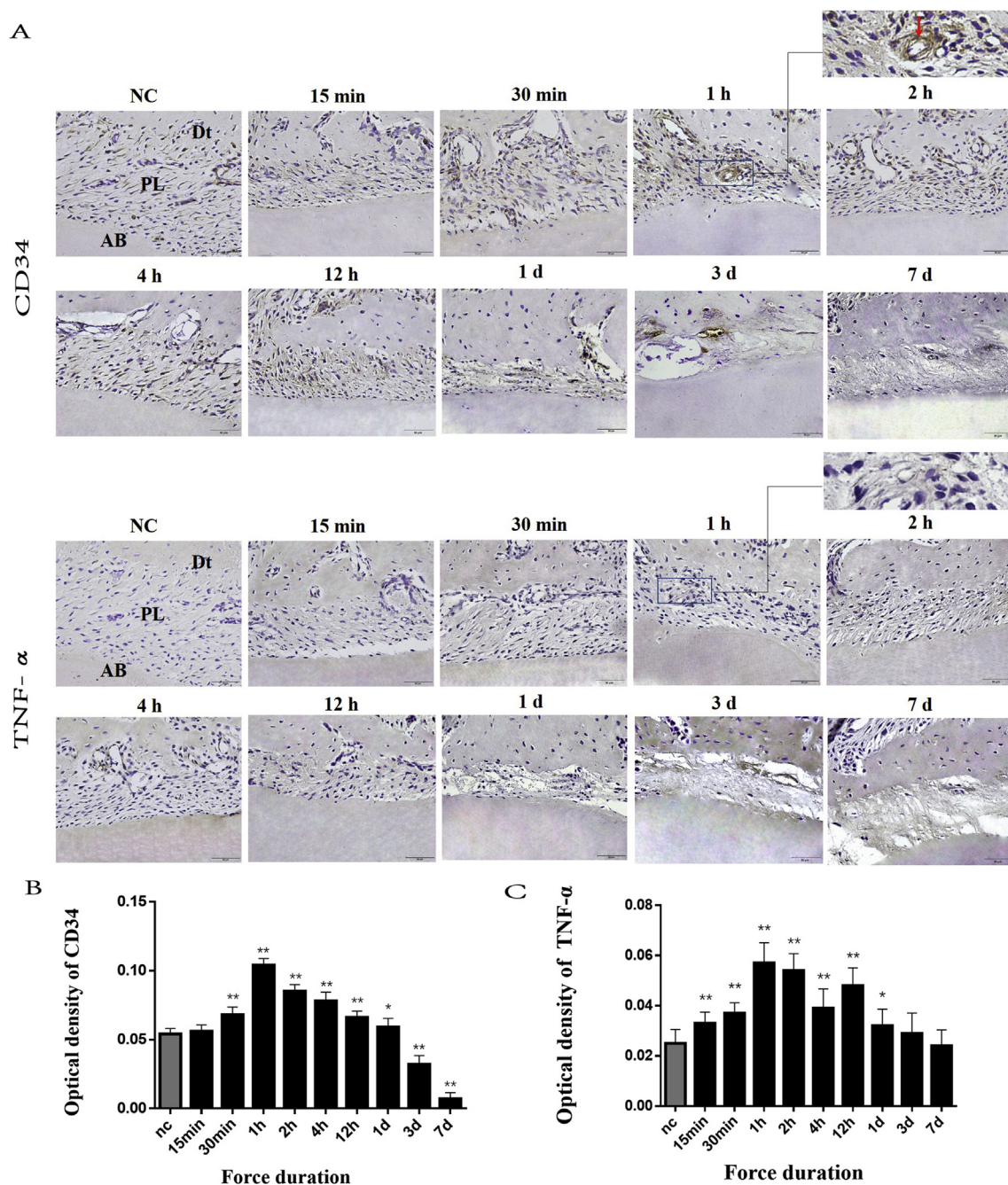
Fig. 6 IHC staining for CD34 and TNF-α in the compression side at different time points. A) Representative images of IHC staining for CD34 and TNF-α. Vascular endothelial marker CD34 mainly expressed around blood vessel, the higher magnification image of the square in the IHC staining image for CD34 at 1 h is shown in the upper right corner panel. Red arrows: the positive cells. TNF-α always diffusely distributed in the extracellular space, so the brown was not as obvious as intracellular proteins. The higher magnification image of the square in the IHC staining image for TNF-α at 1 h is shown in the upper right corner panel. B) Quantitative analysis of IHC staining for CD34 and TNF-α. Scale bars = 50 μm *P < 0.05, **P < 0.01, n = animals 10 per group.

noticeably increased after 1 d of mechanical loading (P < 0.01) and peaked at 7 d (P < 0.01) (Fig. 3B).

IHC staining for autophagy-associated proteins in the compression side of the PDL

IHC staining for beclin-1 and LC3B exhibited very similar trends. Cells expressing LC3B and beclin-1 were present in

all groups, but both LC3B and beclin-1 exhibited a very weak expression pattern in the control group (Fig. 4 and Fig. 5). In the experimental group, the expression of beclin-1 and LC3B fluctuated and gradually increased over time, reaching the highest mean values at 1 h (P < 0.01) before gradually decreasing. In the compression side of the PDL, beclin-1 and LC3B expression increased again to a small peak at 1 d (P < 0.01) and then decreased. Eventually, the
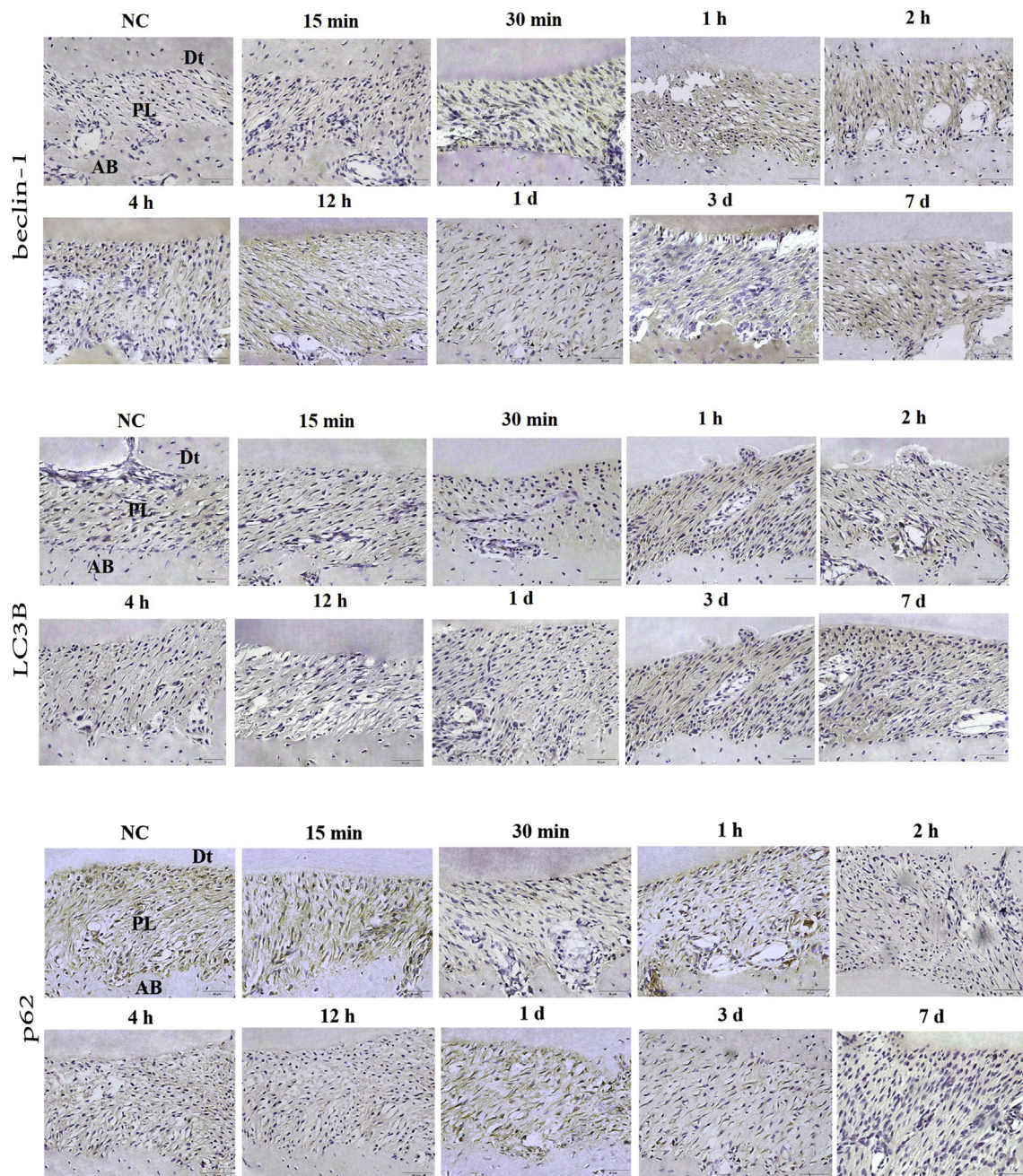
Fig. 7 IHC staining for beclin-1, LC3B and p62/SQSTM1 in the tension side at different time points. Scale bars = 50 μm.

expression of beclin-1 and LC3B decreased to the baseline level at 7 d (P > 0.05). In contrast, IHC staining indicated that p62/SQSTM1 expression followed a completely different trend (Figs. 4 and 5).

### IHC staining for CD34 in the compression side of the PDL

CD34, the most common endothelial cell marker used to evaluate vessel density, is expressed in endothelial cells and individual smooth muscle cells present in arterioles and metarterioles. A significant increase in CD34 expression was observed after mechanical loading (P < 0.01), which

suggests the compression of the blood vessels. Following the adaptation to mechanical stress, CD34 expression gradually decreased. A marked decrease in CD34-positive cells was initially observed at 1 d and finally decreased below the basal level (P < 0.01) (Fig. 6).

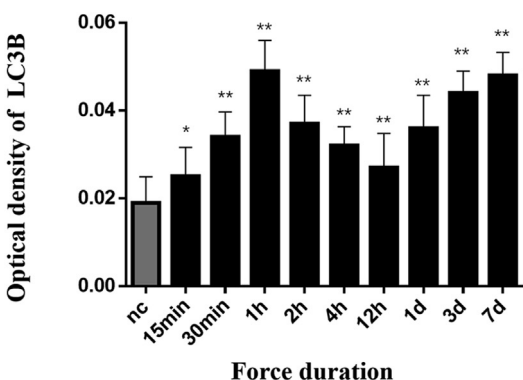### IHC staining for TNF-α in the compression side of the PDL

The levels of TNF-α were maintained to a certain extent in the control group (Fig. 6). After mechanical loading, the levels of TNF-α in the PDL increased continuously until 1 h after mechanical loading. The TNF-α levels then decreased
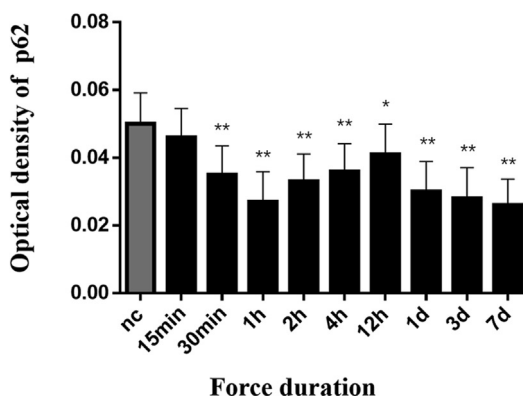
A
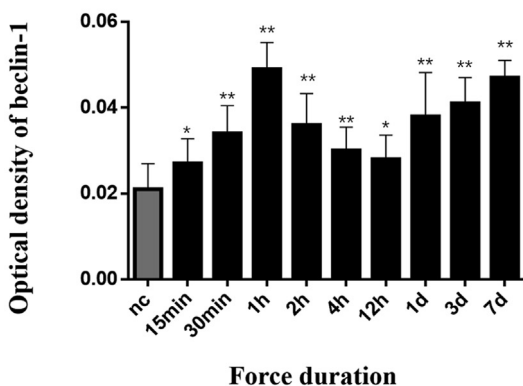
B

C

Fig. 8 Quantitative analysis of IHC staining for beclin-1, LC3B and p62/SQSTM1 in the tension side at different time points. *P < 0.05, **P < 0.01, n = animals 10 per group.

slightly but remained significantly (P < 0.01) higher than the levels in the control group. In the compression side of the PDL, TNF-α expression increased again and peaked at 12 h (P < 0.01) before decreasing. Eventually, TNF-α expression decreased to its baseline level at 7 d.

IHC staining for autophagy-associated proteins in the tension side of the PDL

In the stretched sides of the PDL, the level of autophagy gradually increased and peaked at 1 h (P < 0.01). The autophagy then decreased slightly but remained significantly (P < 0.01) higher than the levels in the control group. With rapid tooth movement observed after 12 h, in the stretched sides of the PDL, autophagy was then increased again at 1 d (P < 0.01), (Fig. 7 and Fig. 8), and continuously increased over time. There was a linear phase of the autophagy level was detected from days 1—7, reaching the highest mean values at 7d (P < 0.01).

IHC staining for TNF-α in the tension side of the PDL

In the tension side of the PDL, the level of TNF-α increased continuously until 1 h after mechanical loading. The TNF-α level then decreased slightly but remained significantly (P < 0.01) higher than the level in the control group. After rapid tooth movement was observed after 12 h, the TNF-α level was increased again at 1 d (P < 0.01) (Fig. 9). There was a linear phase of the TNF-α level was detected from days 1—7, reaching the highest mean values at 7d (P < 0.01), which is the same as the trend of autophagy-associated proteins. In addition, the levels of autophagy and TNF-α expression in the compression side were significantly higher than in the tension side at 2, 4, and 12 h (Fig. 10).

Discussion

Autophagy, a lysosome-based degradation pathway that is reportedly activated by mechanical stress and nutrient deprivation, plays an important role in various physiological and pathological events. Here, autophagy also plays a key role in maintaining the homeostasis and remodeling of periodontal tissue during OTM.[9,22,23]

Under normal conditions, autophagy occurs at a low baseline level to maintain long-term cellular homeostasis. Upon changes in the environment, the autophagy level changes correspondingly.[24] LC3B and beclin-1 are autophagy-related proteins whose levels are correlated with the formation of autophagic vacuoles.[25] Notably, p62/SQSTM1 binds to the autophagosome membrane to degrade target aggregates in autophagosomes.[26] Autophagy activation manifests as an increase in LC3B and beclin-1 levels and the degradation of p62/SQSTM1. In this experiment, autophagy was rapidly activated in the compression side and the tension side of the PDL after mechanical loading, but this increase in autophagy was transient, and the level of autophagy was gradually restored after 1 h. We speculate that this pattern occurs because the PDLCs adapted to the mechanical stress. According to King J S, when mammalian cells are subjected to mechanical stress, autophagy is rapidly induced; while this response is transient, it persists until the cell has remodeled its cortex to relieve the stress.[9] Jiang also reported a half-life of autophagosomes of approximately 8 min. Without persistent stimulation, the autophagy level will return to its normal baseline level after 2 h.[26] In our study, due to the sustained mechanical
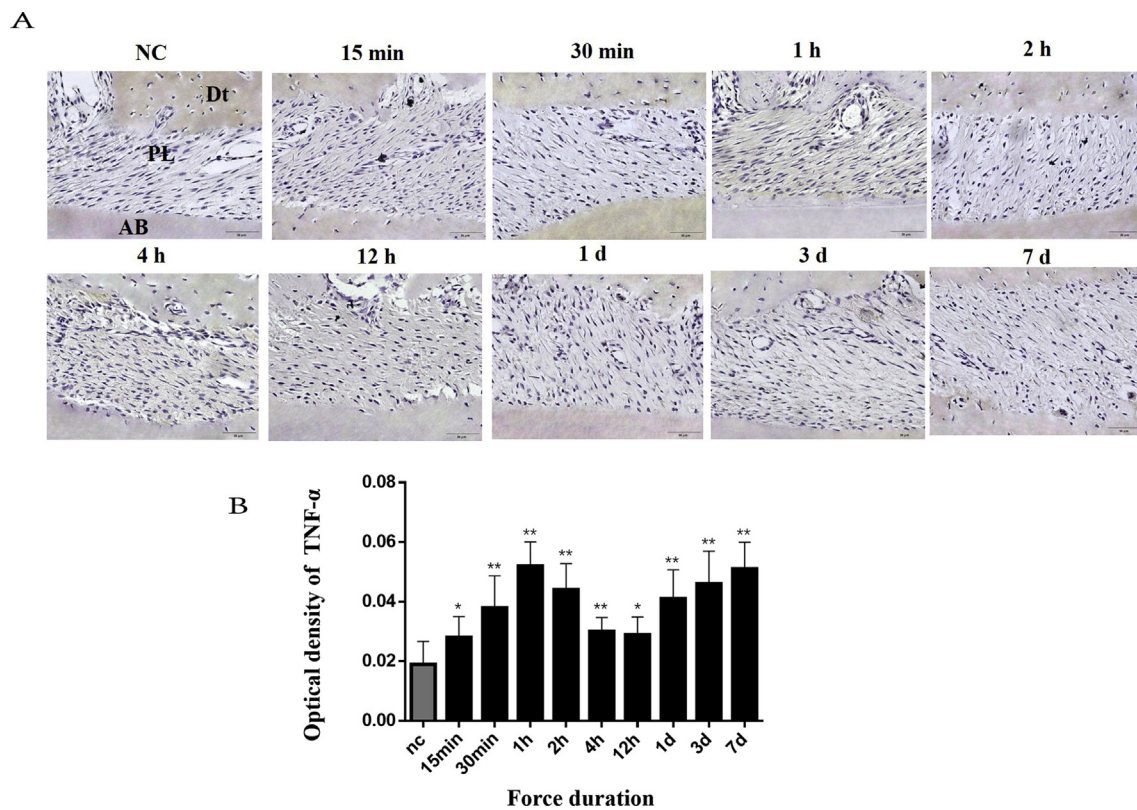
Fig. 9 IHC staining for TNF-α in the tension side at different time points. A) Representative images of IHC staining for TNF-α. B) Quantitative analysis of IHC staining for TNF-α. Scale bars = 50 μm, *P < 0.05, **P < 0.01, n = animals 10 per group.

force, the autophagy level was greater than its baseline level for a longer time.[21] When the autophagy levels between the compression side and the tension side at different time points were compared, the autophagy level in the compression side was significantly greater than in the tension side at 2, 4, and 12 h. The pressure side of the PDL was compressed and narrow after the application of force, which compressed the blood vessels, and CD34 expression was subsequently increased significantly. Due to the substantial compression of the blood vessels, CD34 expression was significantly decreased after 1 h. Therefore, in the present study, the application of a long-term compressive force led to a "starvation" microenvironment that helped to maintain the autophagy level of the PDLCs.

Hyaline degeneration was observed in the pressure side at 1 d, and the number of PDLCs decreased significantly, suggesting that apoptosis occurred. Autophagy is closely related to apoptosis. Under conditions of long-term or high-intensity stimulation, apoptosis often appears in the same cell after autophagy.[10−12,27] Apoptosis, which is triggered in the presence of excess autophagy, has recently been shown to gradually increase over time.[21,28] Therefore, we speculate that the dual effects of starvation and the persistent compression stimulus caused excessive autophagy that amplified apoptosis and mediated the hyaline degeneration in the compression sides of the PDL. Hyalinization may have been absent because apoptosis was not obvious, and bone formation at least partially masked apoptosis in the tension side of the PDL.

Based on the results from the present study, both indirect starvation caused by compressed vessels and direct

force stimulation activated autophagy during OTM, but how is this process achieved? OTM is a sterile inflammatory process. The appropriate inflammatory response is beneficial to the host defenses, but excessive inflammatory responses result in serious damage, such as tissue destruction or organ failure.[29] Autophagy has a wide range of functions with confirmed anti-inflammatory effects.[23,30−32] As shown in the study by Du Li, the activation of inflammasomes induces autophagy, which limits inflammasome activity through physical engulfment.[33] The inhibition of autophagy potentiates inflammasome activity, whereas the stimulation autophagy limited this process. Among the numerous extracellular stimuli that induce autophagy, the role of TNF-α is well established.[34] Hence, we investigated whether the inflammatory cytokine TNF-α is involved in the process regulating autophagy during periodontal tissue remodeling during OTM. TNF-α levels and autophagy exhibited very similar trends, suggesting that TNF-α expression is positively correlated with the initiation of autophagy.

Beclin-1, LC3B, CD34 and TNF-α were all expressed in osteoclasts in the compression side of the PDL. CD34 was expressed in osteoclasts because CD34(+) cells are precursors of osteoclasts;[35] however, why did autophagy occur, and why was TNF-α expressed in osteoclasts? Under hypoxic-ischemic conditions, autophagy is a pivotal regulator of osteoclast differentiation and provides the energy needed for the differentiation and maturation of hypoxia-induced osteoclasts.[5] Additionally, the normal function of osteoclasts requires the participation of TNF-α.[36−38] In the present study, TNF-α levels increased after 12 h, while the
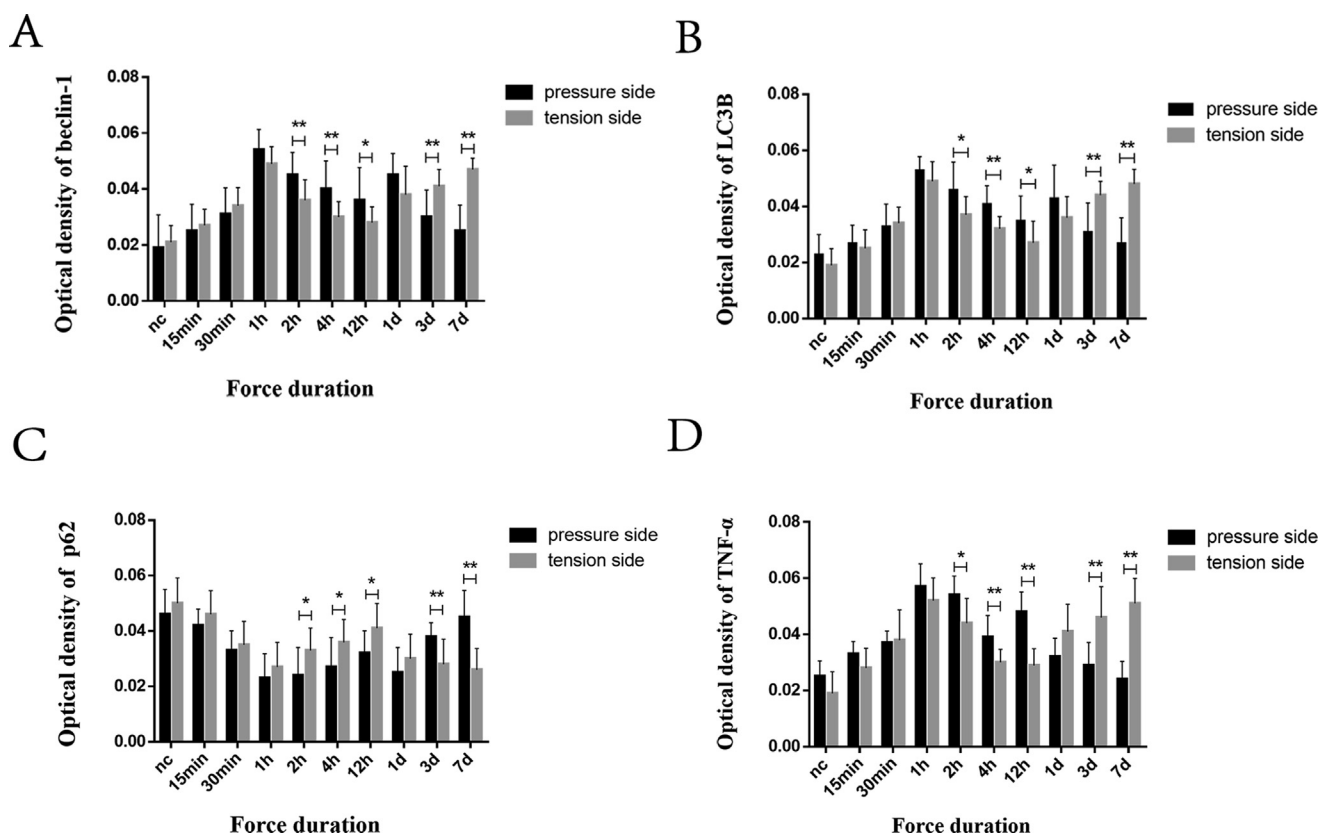
Fig. 10 Comparison of autophagy and TNF-α levels between the compression side and the tension side at different time points. The levels of autophagy and TNF-α expression in the compression side were significantly higher than in the tension side at 2, 4, and 12 h (compression side vs. tension side, *P < 0.05, **P < 0.01, n = 10 animals per group).

number of osteoclasts began to increase at 1 d, and autophagy was obviously observed in osteoclasts at 3 d. These observations might validate the putative participation of autophagy and TNF-α in the regulation of hypoxia-induced osteoclastogenesis. Marino G proposed that autophagy mediates the aggregation of phagocytes and the digestion of necrotic cells.[10] In the present study, the level of autophagy was slightly increased at 1 d. At this time point, osteoclasts began to aggregate around the area of hyalinization, and the number of osteoclasts increased. Thus, autophagy may mediate the recruitment of osteoclasts to the hyaline degeneration zone to ultimately induce bone resorption in the compression side of the PDL. Ravindra Nanda also noted that OTM does not occur as long as these lesions persist.[39] This period is coincident with the unobvious tooth movement phase from 2 h to 12 h. Therefore, once osteoclasts remove necrotic tissue from the compression side of the PDL, the tipping of the dental crown occurs, and the tooth moves quickly at 1 d; therefore, the PDL fibers in the tension zone may be stretched again. Tissue responses at sites of tension tend to occur after tissue removal at compression sites. These findings might explain the occurrence of autophagy and the upregulation of TNF-α expression in the tension zone after 12 h. Finally, further investigations are needed to determine whether autophagy and TNF-α mediate bone formation in the tension side of the PDL,

along with the presence of osteoblasts and related proteins.

Taken together, autophagy mediates hyaline degeneration in the PDL, affects the biological functions of osteoclasts, and promotes the maintenance of cell metabolism and survival. A significant correlation between the initiation of autophagy and TNF-α expression is observed, both of which exert a positive effect on PDL remodeling during OTM in rats. However, in the present study, due to the limitations of in vivo experiments, the overlapping effects of mechanical force and starvation on autophagy in PDLCs were not clearly distinguished. Further studies are needed to obtain a better understanding of this process.

Declaration of Competing Interest

None.

References

1. Westover L, Faulkner G, Flores-Mir C, Hodgetts W, Raboud D. Non-invasive evaluation of periodontal ligament stiffness during orthodontic tooth movement. *Angle Orthod* 2019;89: 228—34.

2. Ma KG, Shao ZW, Yang SH, et al. Autophagy is activated in compression-induced cell degeneration and is mediated by reactive oxygen species in nucleus pulposus cells exposed to compression. *Osteoarthritis Cartilage* 2013;21:2030—8.

3. Dutra EH, Nanda R, Yadav S. Bone response of loaded periodontal ligament. *Curr Osteoporos Rep* 2016;14:280—3.

4. Dupont N, Codogno P. Autophagy transduces physical constraints into biological responses. *Int J Biochem Cell Biol* 2016; 79:419—26.

5. Meikle MC. The tissue, cellular, and molecular regulation of orthodontic tooth movement: 100 years after Carl Sandstedt. *Eur J Orthod* 2006;28:221—40.

6. Kourtis N, Tavernarakis N. Autophagy and cell death in model organisms. *Cell Death Differ* 2009;16:21—30.

7. Galluzzi L, Pietrocola F, Levine B, Kroemer G. Metabolic control of autophagy. *Cell* 2014;159:1263—76.

8. Kroemer G, Mariño G, Levine B. Autophagy and the integrated stress response. *Mol Cell* 2010;40:280—93.

9. King JS, Veltman DM, Insall RH. The induction of autophagy by mechanical stress. *Autophagy* 2011;7:1490—9.

10. Mariño G, Niso-Santano M, Baehrecke EH, Kroemer G. Self-consumption: the interplay of autophagy and apoptosis. *Nat Rev Mol Cell Biol* 2014;15:81—94.

11. Meng Y, Ji J, Tan W, et al. Involvement of autophagy in the procedure of endoplasmic reticulum stress introduced apoptosis in bone marrow mesenchymal stem cells from non-obese diabetic mice. *Cell Biochem Funct* 2016;34:25—33.

12. Oral O, Akkoc Y, Bayraktar O, Gozuacik D. Physiological and pathological significance of the molecular cross-talk between autophagy and apoptosis. *Histol Histopathol* 2016;31:479—98.

13. Mizushima N, Klionsky DJ. Protein turnover via autophagy: implications for metabolism. *Annu Rev Nutr* 2007;27:19—40.

14. Yang Y, Gao J, Zhang Y, et al. Natural pyrethrins induce autophagy of HepG2 cells through the activation of AMPK/m-TOR pathway. *Environ Pollut* 2018;241:1091—7.

15. Huang Z, Fang W, Liu W, et al. Aspirin induces Beclin-1-dependent autophagy of human hepatocellular carcinoma cell. *Eur J Pharmacol* 2018;823:58—64.

16. He C, Klionsky DJ. Regulation mechanisms and signaling pathways of autophagy. *Annu Rev Genet* 2009;43:67—93.

17. Adiseshaiah PP, Skoczen SL, Rodriguez JC, Potter TM, Kota K, Stern ST. Autophagy monitoring Assay II: imaging autophagy induction in LLC-PK1 cells using GFP-LC3 protein fusion construct. *Methods Mol Biol* 2018;1682:211—9.

18. Ye J, Jiang Z, Chen X, Liu M, Li J, Liu N. The role of autophagy in pro-inflammatory responses of microglia activation via mitochondrial reactive oxygen species in vitro. *J Neurochem* 2017;142:215—30.

19. Shi CS, Shenderov K, Huang NN, et al. Activation of autophagy by inflammatory signals limits IL-1β production by targeting ubiquitinated inflammasomes for destruction. *Nat Immunol* 2012;13:255—63.

20. Wellnitz K, Taegtmeyer H. Mechanical unloading of the failing heart exposes the dynamic nature of autophagy. *Autophagy* 2010;6:155—6.

21. Lin FY, Hsiao FP, Huang CY, et al. Porphyromonas gingivalis GroEL induces osteoclastogenesis of periodontal ligament cells and enhances alveolar bone resorption in rats. *PloS One* 2014; 9:e102450.

22. Xi G, Rosen CJ, Clemmons DR. IGF-I and IGFBP-2 stimulate AMPK activation and autophagy, which are required for osteoblast differentiation. *Endocrinology* 2016;157:268—81.

23. Levine B, Mizushima N, Virgin HW. Autophagy in immunity and inflammation. [J]. *Nature* 2011;469:323—35.

24. Nollet M, Santucci-Darmanin S, Breuil V, et al. Autophagy in osteoblasts is involved in mineralization and bone homeostasis. *Autophagy* 2014;10:1965—77.

25. Grootaert MO, da Costa Martins PA, Bitsch N, et al. Defective autophagy in vascular smooth muscle cells accelerates senescence and promotes neointima formation and atherogenesis. *Autophagy* 2015;11:2014—32.

26. Jiang Y, Kou J, Han X, et al. ROS-dependent activation of autophagy through the PI3K/Akt/mTOR pathway is induced by hydroxysafflor yellow A-sonodynamic therapy in THP-1 macrophages. *Oxid Med Cell Longevity* 2017;2017:8519169s.

27. Puente C, Hendrickson RC, Jiang X. Nutrient-regulated phosphorylation of ATG13 inhibits starvation-induced autophagy. *J Biol Chem* 2016;291. 6026-35.

28. Liu F, Wen F, He D, et al. Force-induced H2S by PDLSCs modifies osteoclastic activity during tooth movement. *J Dent Res* 2017; 96:694—702.

29. Bharath LP, Mueller R, Li Y, et al. Impairment of autophagy in endothelial cells prevents shear-stress-induced increases in nitric oxide bioavailability. *Can J Physiol Pharmacol* 2014;92: 605—12.

30. Deretic V, Saitoh T, Akira S. Autophagy in infection, inflammation and immunity. *Nat Rev Immunol* 2013;13:722—37.

31. Cappelletti C, Galbardi B, Kapetis D, et al. Autophagy, inflammation and innate immunity in inflammatory myopathies. *PloS One* 2014;9:e111490.

32. Ge Y, Huang M, Yao YM. Autophagy and proinflammatory cytokines: interactions and clinical implications. *Cytokine Growth Factor Rev* 2018;43:38—46.

33. Du L, Li Y, Liu W. Maresin 1 regulates autophagy and inflammation in human periodontal ligament cells through glycogen synthase kinase-3β/β-catenin pathway under inflammatory conditions. *Arch Oral Biol* 2017;87:242—7.

34. Cheng Y, Qiu F, Tashiro S, Onodera S, Ikejima T. ERK and JNK mediate TNFα-induced p53 activation in apoptotic and autophagic L929 cell death. *Biochem Biophys Res Commun* 2008; 376:483—8.

35. Wu DJ, Adamopoulos IE. Autophagy and autoimmunity. *Clin Immunol* 2017;176:55—62.

36. Mo S, Hua Y. Cystathionine gamma lyase-H2S contributes to osteoclastogenesis during bone remodeling induced by mechanical loading. *Biochem Biophys Res Commun* 2018;501: 471—7.

37. Arai C, Nomura Y, Matsuzawa M, Hanada N, Nakamura Y. Extracellular HSP72 induces proinflammatory cytokines in human periodontal ligament fibroblast cells through the TLR4/NFκB pathway in vitro. *Arch Oral Biol* 2017;83:181—6.

38. Kimura M, Nagai T, Matsushita R, Hashimoto A, Miyashita T, Hirohata S. Role of FK506 binding protein 5 (FKBP5) in osteoclast differentiation. *Mod Rheumatol* 2013;23:1133—9.

39. Nanda R. *Biomechanics and esthetic strategies in clinical orthodontics*, 1nd ed. Connecticut: Farmington; 2005:17—25.